Cancer Letters 448 (2019) 61–69

Contents lists available at ScienceDirect

Cancer Letters

journal homepage: www.elsevier.com/locate/canlet

Original Articles

Knock-down of oncohistone H3F3A-G34W counteracts the neoplastic phenotype of giant cell tumor of bone derived stromal cells

J. Fellenberg[a,*], H. Sähr[a], D. Mancarella[b], C. Plass[b], A.M. Lindroth[c], F. Westhauser[a], B. Lehner[a], V. Ewerbeck[a]

[a] Center for Orthopedics, Trauma Surgery and Spinal Cord Injury, Heidelberg University Hospital, Heidelberg, Germany
[b] Division of Epigenomics and Cancer Risk Factors, German Cancer Research Center (DKFZ), Heidelberg, Germany
[c] Graduate School of Cancer Science and Policy, Cancer Biomedical Science, National Cancer Center, Gyeonggi-do, Republic of Korea

ARTICLE INFO

Keywords:
Giant cell tumor of bone
Histone
H3.3-G34W
Neoplastic transformation
CAM assay

ABSTRACT

Giant cell tumors of bone (GCTB) are semi-malignant tumors associated with extensive osteolytic defects and massive bone destructions. They display a locally aggressive behavior and a very high recurrence rate. Recently, a single mutation has been identified in GCTB affecting the *H3F3A* gene coding for the histone variant H3.3 (H3.3-G34W). The aim of this study was to investigate whether H3.3-G34W is sufficient to drive tumorigenesis in GCTB. Initially, we confirmed the high frequency of this mutation in 94% of 84 analyzed tissue samples. Using a siRNA based approach we could selectively knockdown H3.3-G34W in primary neoplastic stromal cells isolated from tumor tissue (GCTSC). H3.3-G34W knockdown caused a significant inhibition of cell proliferation, migration and colony formation capacity *in vitro*. Xenotransplantation of GCTSCs onto the chorioallantoic membrane of fertilized chicken eggs further demonstrated a significant impact of H3.3-G34W knockdown on tumor engraftment and growth *in vivo*. Our data indicate that H3.3-G34W is sufficient to drive tumorigenesis in GCTB. Apart from the application of H3.3-G34W screening as diagnostic tool, our data suggest that H3.3-G4W represents a promising target for the development of new GCTB therapies.

1. Introduction

Giant cell tumors of bone (GCTB) are semi-malignant neoplasms predominantly affecting the meta- and epiphyseal regions of the long bones. They represent 5% of all bone tumors and occur mainly in young adults aged 20–40 years [1,2]. GCTBs are characterized by a very high recurrence rate ranging from 20 to 55% depending on the surgical technique and the use of adjuvants [3]. They are composed of neoplastic stromal cells, osteoclast-like multinucleated giant cells and macrophage like giant cell precursors. Recently, a single driver mutation has been identified in GCTB affecting the *H3F3A* gene, one of two genes (*H3F3A* and *H3F3B*) encoding the histone variant H3.3 [4]. The identified point mutation causes a glycin to tryptophan substitution at position 34 (H3.3-G34W) and is restricted to the neoplastic stromal cell population. As part of nucleosomes, histones are crucially involved in chromatin condensation and maintenance of chromatin structure, thus influencing genomic stability and transcriptional regulation. The N-terminal tails of histone proteins are frequently altered by post-transcriptional modifications including methylation, acetylation and phosphorylation that influence DNA binding characteristics and represent binding domains for further regulatory factors [5,6]. Most known histone mutations are located in or near posttranslational modification sites, thus preventing successful histone modification. The consequences are massive alterations within the epigenomic landscape and the gene expression profiles of affected cells [7] (Plass et al. unpublished). Although mutations in histone coding genes occur heterozygously with one or more wildtype copies remaining, they are able to drive tumorigenesis and are thus also termed oncohistones. Histone mutations are preferentially found in the H3.3 variant and affect one of the N-terminal amino acids K27, K36 or G34. In contrast to the canonical variants H3.1 and H3.2 that are expressed only during the S-phase of the cells cycle, H3.3 synthesis is replication independent and deposition occurs throughout the cell cycle. A chaperone complex consisting of DAXX (death-domain associated protein) and ATRX (alpha-thalssaemia/mental retardation syndrome X-linked) incorporates H3.3 into pericentromeric and telomeric heterochromatin while a second

Abbreviations: GCTB, giant cell tumor of bone; GCTSC, giant cell tumor derived stromal cells; CAM, chorionallantoic membrane

* Corresponding author. Center for Orthopedics, Trauma Surgery and Spinal Cord Injury, Heidelberg University Hospital, Schlierbacher Landstraße 200a, 69118, Heidelberg, Germany.
E-mail address: joerg.fellenberg@med.uni-heidelberg.de (J. Fellenberg).

https://doi.org/10.1016/j.canlet.2019.02.001
Received 31 October 2018; Received in revised form 24 January 2019; Accepted 1 February 2019

chaperone complex HIRA incorporates H3.3 into actively transcribed euchromatic regions [8,9]. H3.3 mutations are frequently found in pediatric brain and bone tumors and have been shown to be tumor type specific. H3.3-K27M is frequently found in pediatric glioma [10] and H3.3-K36M is common in chondroblastoma [4] and head and neck squamous cell carcinoma [11]. Mutations in HIST1H1B-E genes coding for the linker histone H1 have been detected in non-Hodgkin lymphoma [12] and in rare cases mutations in *H3F3A* encoding G34 W/R substitutions have been observed in osteosarcoma [13]. GCTBs are characterized by a high incidence of mutations within the *H3F3A* gene encoding H3.3_G34W and to a much lesser extent by a glycine to leucine substitution (H3.3-G34L) [4]. Due to this specificity, detection of H3.3-G34W has been successfully applied as diagnostic tool for the identification of GCTBs and their distinction from histologic mimics like chondroblastoma, aneurysmal bone cysts and giant cell rich osteosarcoma variants [14,15].

In this study, the relevance of the oncohistone H3.3-G34W for the neoplastic transformation of GCTB stromal cells (GCTSCs) was investigated *in vitro* and *in vivo* using a siRNA-mediated knockdown approach.

2. Materials and methods

The use of patient tissue-derived cell lines was approved by the Ethics Committee of the University of Heidelberg and informed consent to analyze tumor tissue and to publish clinical details was obtained from all individuals included in the study.

2.1. Sample preparation and cell culture

Primary GCTSCs were isolated from tissue samples derived from tumor resections in our clinic. The tissue was mechanically cut in small pieces and digested with 1.5 mg/ml collagenase B (Roche Diagnostics, Mannheim, Germany) for 3 h at 37 °C in Dulbecco's Modified Eagle Medium (DMEM) (Lonza GmbH, Köln, Germany) containing 4.5 g/l glucose and supplemented with 10% fetal calf serum (FCS) (Biochrom, Berlin, Germany), and 100 U/ml penicillin/streptomycin (Lonza). Cells were collected by centrifugation, washed twice in PBS and cultured in DMEM. Twenty-four hours after plating, cells were carefully treated with Trypsin/EDTA (Lonza) leaving the giant cells attached in the culture flask. Detached cells were cultured for further 3 passages eliminating any remaining giant cells and histiocytes.

2.2. H3F3A-G34W knock-down

Knock-down of mutated H3F3A-G34W was achieved by transient transfection of H3F3A-G34W siRNAs. Three siRNAs were designed as 19-nucleotide duplexes with a 3′-dTdT overhang (Eurofins Genomics, Ebersberg, Germany). SiRNAs differed in the position of the mutated nucleotide (position 12–14): siG34W-12 5′-UUUCUUCACCC**A**UCCA GUA-3′; siG34W-13 5′-GUUUCUUCACCC**A**UCCAGU-3′; siG34W-14 5′-GGUUUCUUCACCC**A**UCCAG-3′. Transfection of GCTSCs was done by electroporation. As controls, cells were either mock transfected without the addition of siRNA or cells were transfected with a negative control siRNA (Mission siRNA negative Control #1) (Sigma-Aldrich, Taufkirchen, Germany). Transfection was carried out with the electroporation unit MP-100 (VWR International GmbH, Darmstadt, Germany). Cells were cultured until they reached ~80% confluence, trypsinized and washed twice in PBS. For transfection, 10^6 cells were resuspended in 100 µl R-buffer containing 5 µM siRNA. After electroporation with two pulses at 1300 V for 15 ms, cells were plated in DMEM-medium and cultured for 48 h before they were used for the different assays.

2.3. RNA extraction

Total RNA was extracted using mirVana miRNA Isolation Kit (Invitrogen, Darmstadt, Germany). RNA concentrations and purities were determined with a NanoDrop ND-1000 spectrophotometer (VWR).

2.4. DNA extraction

Extraction of genomic DNA from tumor tissue and cell lines was done using the Quick DNA Plus kit (Zymo Research, Freiburg, Germany) according to the manufacturer instructions. DNA concentrations and purities were determined with a NanoDrop ND-1000 spectrophotometer (VWR).

2.5. Detection of the H3F3A mutation by polymerase chain reaction

Detection of the H3F3A-G34W mutation by polymerase chain reaction was done using forward primer specific for the mutated and the wild-type sequence, respectively, in combination with a unique reverse primer. The following primers were used:

H3F3A-wild-type 5′-AGTGCGCCCTCTACTGGAG-3′; H3F3A-G34W 5′-AGTGCGCCCTCTACTGGAT-3′; H3F3A-reverse 5′-CTCCAGGTAAGA TTATGGCTTC-3′. Amplification was performed using 100 ng genomic DNA as template, 0.25 µl PlatinumTaq polymerase (Invitrogen), 0.6 µl $MgCl_2$ (50 mM), 0.4 µl dNTPs (10 mM each) and 0.5 µl of each primer (10 µM) in a total volume of 20 µl. Samples were incubated at 94 °C for 3 min followed by 36 cycles of denaturation at 94 °C for 15 s, annealing at 66 °C for 30 s and extension at 72 °C for 45 s and a final extension step at 72 °C for 7 min. PCR products were separated on a 1.6% agarose gel and visualized by Midori Green (Biozym, Hessisch Oldendorf, Germany) staining.

2.6. Detection of the H3F3A mutation by restriction site mutation analysis

Genomic DNA was used as template for PCR amplification of a 368 bp fragment covering the H3F3A-G34W locus. Samples were incubated at 94 °C for 3min followed by 36 cycles of denaturation at 94 °C for 15 s, annealing at 58 °C for 30 s and extension at 72 °C for 45 s and a final extension step at 72 °C for 7 min. The following primers were used: H3F3A-RF 5′-GTCTCTGTACCATGGCTCGT-3′; H3F3A-reverse 3′-CTCC AGGTAAGATTATGGCTTC-5′. After the PCR amplification 4 U of the restriction enzyme *Bse*GI were added (Fisher Scientific, Schwerte, Germany) and the samples were further incubated at 55 °C for 90 min and separated on a 1.6% agarose gel stained with Midori Green (Biozym).

For the detection of the H3F3A-G34W mutations in expressed H3F3A transcripts cDNA was generated from 1 µg total RNA using 1 µl Omniscript (Qiagen, Hilden, Germany), 10 µM oligo-dT primer, 5 mM dNTPs and 10 U RNaseOut (Invitrogen) for 2 h at 37 °C in a total volume of 20 µl. PCR amplification of the H3F3A transcripts was done as described above using the following primer: H3F3A-F3 5′-ATCAAGTTGT CTACGGCGGA-3′; H3F3A-R3 5′-TGGATAGCACACAGGTTGGT-3′. After addition of 4 U of the restriction enzyme *Bse*GI and incubation at 55 °C for 90 min, restriction fragments were separated in a 1.6% agarose gel stained with Midori Green (Biozym) and photographed. Densitometric quantification was performed using BIO-ID software version 15.01 (Vilber Lourmat, Eberhardzell, Germany).

2.7. RT-qPCR

First strand complementary DNA (cDNA) was synthesized from 1 µg of total RNA using 1 µl Omniscript (Qiagen, Hilden, Germany), 10 µM oligo-dT primer, 5 mM dNTPs and 10 U RNaseOut (Invitrogen, Karlsruhe, Germany) for 1.5 h at 37 °C in a total volume of 20 µl. After synthesis cDNA was further diluted 1:10 with 10 mM Tricine. RT-qPCR was performed in the real-time thermal cycler Mx3000p (Agilent

Technologies, Waldbronn, Germany) in a total volume of 20 µl using Absolute QPCR SYBR Green mix (Thermo scientific, Dreieich, Germany) and 2 µl of cDNA as template. Samples were heated to 95 °C for 15 min followed by 40 cycles of denaturation at 95 °C for 15 s, annealing at 58 °C for 20 s and extension at 72 °C for 30 s. After the last cycle, a melting curve analysis was performed to verify the specificity of the amplified PCR products. Calculated gene expression was normalized on the basis of the expression of RPS13 (ribosomal protein S13) in the corresponding sample. The following primers were used: RPS13-F 5′-GGTTGAAGTTGACATCTGACGA-3′; RPS13-R 5′- CTTGTGCAACACC ATGTGAAT -3′; RANKL-F 5′-AGCTCAGCCTTTTGCTCATC -3′; RANKL-R 5′—CCATTGCTAAAAGTCATGTTGG -3.

2.8. Western blot

Five µg of total protein were separated on a 12% polyacrylamide gel and transferred to Immobilon-P membranes (Millipore, Schwalbach, Germany). After blocking with PBS supplemented with 5% skim milk (Sigma-Aldrich) and 0.05% Tween 20 (Sigma-Aldrich) membranes were incubated overnight at 4 °C with one of the following primary antibodies at the indicated dilutions: Aktin (1:5000) (BD Biosciences, Heidelberg, Germany), Histone H3.3 (1:500) (Merck Chemicals, Darmstadt, Germany), Histone H3 pan (1:20000) (Merck Chemicals GmbH) H3.3 G34W (1:1000) (Active Motiv, Carlsbad, USA). After washing three times in PBS containing 0.1% Tween 20 membranes were incubated for 1 h at room temperature with 5000-fold diluted peroxidase conjugated secondary antibody (Biozol, Eching, Germany). Proteins recognized by the antibody were visualized with Clarity western ECL substrate (Bio-Rad Laboratories GmbH, München, Germany) according to the manufacturer's instructions. Signal intensities were quantified by densitometry using Bio-1D software version 15.01 (Vilber Lourmat, Eberhardzell, Germany).

2.9. Immunohistochemistry

Formalin fixed, paraffin embedded GCT tissue sections were deparaffinized in Roti-Histol (Carl Roth, Karlsruhe, Germany) and rehydrated with isopropanol. Antigen retrieval was performed using Dako target retrieval buffer pH 6 (Dako, Hamburg, Germany) in a high pressure cooker at 121 °C for 5 min. Sections were blocked with PBS supplemented with 5% BSA before primary antibodies diluted in PBS/5% BSA were applied and incubated over night at 4 °C. For detection of all histone H3 variants an anti-histone H3 primary antibody (Merck Chemicals) and for the detection of mutated H3F3A-G34W a H3.3G34W antibody (RevMab Biosciences, San Francisco, USA) were used at a dilution of 1:1000. Detection was done using the BrightVision plus kit (VWR) according to manufacturer's instructions. ImmPACT Vector Red (Linaris, Dossenheim, Germany) was used as substrate. Samples were counterstained with hematoxylin and mounted with NeoMount (VWR).

2.10. Proliferation assay

For the analysis of cell proliferation 5×10^3 cells were seeded in a 96-well plate 48 h after transfection, cultured in DMEM medium containing 10% FCS and counted after 0, 3, 4, 5, 6 and 9 days using a MACSQuant flow cytometer (Miltenyi Biotec, Bergisch Gladbach, Germany). All analyses were done in triplicates.

2.11. Migration assay

Cell migration was measured using the Oris™ 96-well cell migration assay kit (Platypus Technologies, Madison, USA) following the manufacturer's instructions. In brief, 2×10^4 cells were seeded in 96-well plates in which cell-seeding stoppers were inserted. These stoppers prevent the attachment of cells within a defined detection zone of 2 mm diameter in the middle of each well. After 24 h the cell seeding stoppers were removed and the cells were washed with PBS. Cells were cultured in DMEM for further 72 h to allow migration, washed with PBS, stained with PBS supplemented with 1 µM calcein-AM at 37 °C for 15 min and photographed. The area of migrated cells within the detection zone was quantified using ImageJ software (National Institutes of Health, Bethesda, Maryland, USA).

2.12. Soft agar colony formation assay

Cells were trypsinized, counted and 3×10^4 cells were resuspended in 300 µl DMEM containing 0.3% agar, 10% FCS and 100 U/ml penicillin/streptomycin at a temperature of 42 °C. The cells suspensions were layered on top of 0.5% agar in 24-well plates and incubated at ambient temperature until the agar was hardened. After addition of 1 ml DMEM the cells were incubated at 37 °C in a humidified incubator for 28 days. Colonies containing > 20 cells were counted under a microscope. Experiments were done in triplicates with three different GCTSC cell lines.

2.13. Chicken chorionallantois membrane assay

Fertilized white Leghorn chicken eggs were delivered by a local ecological hatchery (Geflügelzucht Hockenberger, Eppingen, Germany). Upon delivery eggs were cleaned and incubated in an upright position at a humidity of 70%, a temperature of 37.8 °C and permanent agitation. This time point was designated as embryonic development day 0 (EDD 0). At EDD 4, eggs were prepared for transplantation by horizontal positioning of the eggs and removal of 3 ml albumen. A Leukosilk tape (BSN medical, Hamburg, Germany) was applied on the upper side of the egg before the chorioallantoic membrane was exposed by cutting a window of approximately 1.5 cm diameter into the eggshell. Transplantation of tumor cells (2×10^6 cells/egg in 30 µl) was performed at EDD 9. The window was opened again and a sterile silicone ring (9 mm inner diameter) was placed onto the CAM. The CAM area within this ring was gently lacerated using a 30 gauge needle before the cells were inoculated. Cells were resuspended in DMEM medium mixed with an equal amount of the matrix Cultrex BME Type 3 (AMS Biotechnology, Frankfurt, Germany) and inoculated onto the CAM. Seven days post transplantation at EDD 16 the xenograft tumors were resected after humane euthanasia of the chick embryo by injection of 50 µl (16 g/100 ml) of the pentobarbital Narcoren® (Merial, Hallbergmoos, Germany) into the chicken vasculature. Embryos that died before EDD 16 were excluded from the study. The volumes of the excised tumors were estimated using the following formula: volume = 4/3 × pi × r3 (r = 1/2 × √ of diameter 1 × diameter 2). Tumor take rates were calculated as: number of eggs with tumors *100/number of eggs with vital embryos. All experiments were conducted at least in duplicates.

2.14. Data analysis and statistics

Statistical analyses were conducted using SPSS Statistics, version 22 (IBM, Armonk, USA). Descriptive statistics such as means, standard deviations and medians were calculated. Comparisons of two groups were performed by the Mann Whitney *U* test for independent groups. The Pearson's chi-squared test was used to analyze nominal data. For all statistic calculations p-values below 0.05 were considered statistically significant. Reported p-values are two-sided.

3. Results

3.1. GCTB tissue and stromal cell lines are characterized by a recurrent, heterozygous mutation in the H3F3A gene encoding the oncohistone H3.3-G34W

An initial screening for the H3.3-G34W encoding mutation in

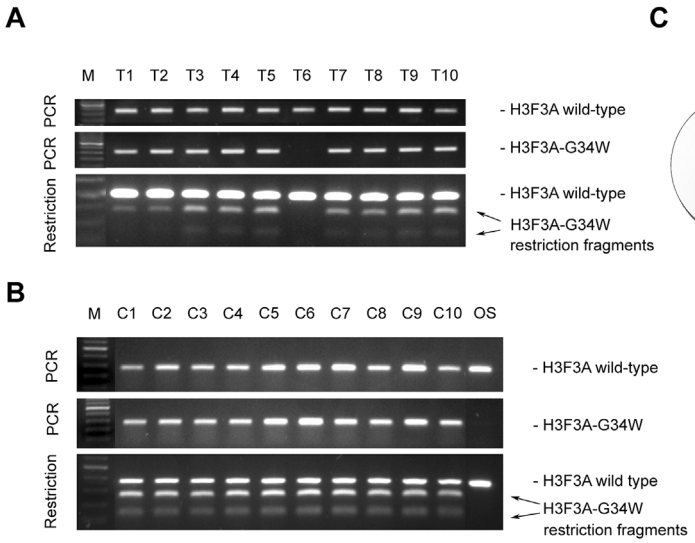

Fig. 1. A recurrent H3F3A mutation can be detected in GCTB. **(A)** Genomic DNA from 84 GCTB tissue samples has been subjected to H3F3A screening by PCR and *Bse*GI restriction site mutation analysis. Results from 10 representative samples are shown confirming the existence of a wild type and a G34W mutated allele in the majority of the analyzed samples. **(B)** Screening of GCTSC cell lines isolated from GCT tissue showing the H3F3A mutation in all cell lines (OS = osteosarcoma cell line Saos-2). **(C)** Summary of G34W screening in 84 GCTB tissue samples.

H3F3A was performed using genomic DNA isolated from 84 GCTB tissue samples by mutation specific PCR and restriction site mutation analysis. With both methods the heterozygous mutation could be detected in 79 cases (94%) (Figire 1 A). All stromal GCTB cell lines established from H3.3 G34W positive tissues carried the mutation as well, while a control osteosarcoma cell line (Saos-2) was negative (Fig. 1 B). One GCT patient carried the rare G34L mutation (Lutsik et al. unpublished). (Fig. 1C).

3.2. H3F3A-G34W is restricted to the neoplastic stromal cell population

GCTBs are characterized by a large amount of multinucleated giant cells that can easily be visualized in tissue sections due to their expression of tartrate resistant acid phosphatase (TRAP). Immunohistochemical staining for TRAP and H3.3-G34W in serial sections of GCTB tissues showed a strong H3.3-G34W signal in the GCTSC population which has previously been identified as the neoplastic component of GCTB. Multinucleated giant cells were negative for H3.3 G34W (Fig. 2).

3.3. Specific siRNA mediated knockdown of the mutated H3F3A allele

To analyze the relevance of the mutant histone variant H3.3-G34W for the neoplastic transformation of GCTSCs, a siRNA mediated knockdown approach was used. To achieve optimal knockdown of H3.3-G34W we initially designed three siRNAs directed against the mutated allele of *H3F3A* with the mutated nucleotide located at position 12, 13 and 14, respectively. Knockdown efficiencies were investigated by transient transfection of a GCTSC cell line and subsequent Western blot analysis of total H3 and mutated H3.3-G34W protein levels. While siG34W-12 and siG34W-13 only slightly decreased H3.3-G34W expression, a nearly complete knockdown was achieved by siG34W-14. In contrast, total H3 expression was unaffected by all siRNAs tested (Fig. 3A). Based on these results the siRNA siG34W-14 was used for all further experiments. We verified the knockdown of H3.3-G34W in all individual cell lines used for further experiments by western blot and restriction site mutation analysis and subsequent densitometric quantification. To ensure that knockdown was sufficient during the whole period of experimentation, quantification was carried out 12 days after transient transfection of the cells. Consistent with the fact that H3.3-G34W represents only a small fraction of total H3 proteins, H3.3-G34W knockdown induced only a minor reduction of total H3 proteins to 84% compared to mock transfected cells. Levels of the histone H3 variant H3.3 (wild-type and mutant) were reduced to 62% compared to mock transfected cells reflecting the fact that H3.3 is encoded by two genes and only one of the four alleles is mutated in GCTB.

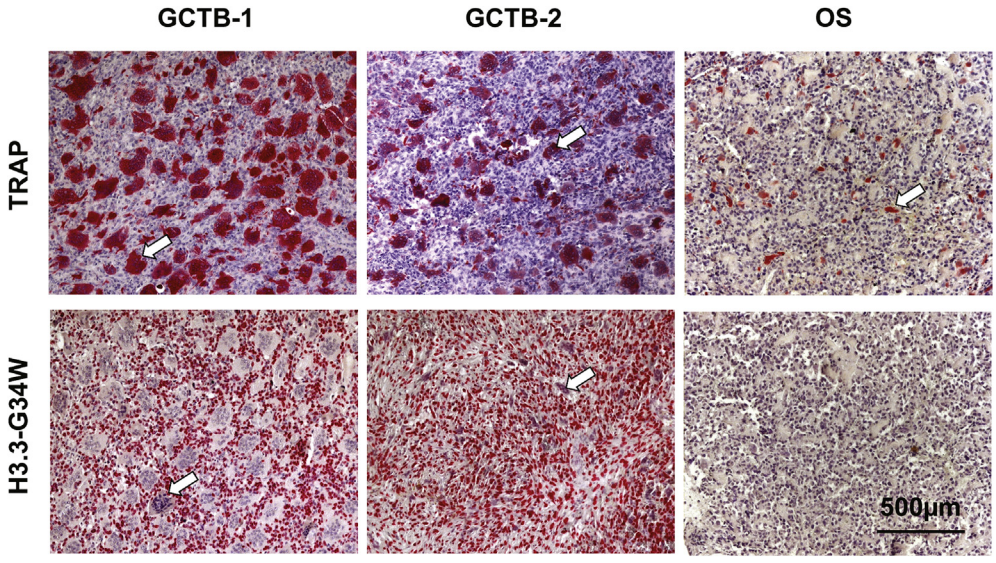

Fig. 2. H3.3-G34W is restricted to GCTSCs. Immunohistochemical analysis of tartrate resistant acid phosphatase (TRAP) expressed by multinucleated giant cells and expression of H3.3-G34W in GCTB tissues. Positive staining is shown in red and sections were counterstained with hematoxylin (blue). Multinucleated giant cells are indicated by arrows. An osteosarcoma tissue section served as H3.3-G34W negative control. (For interpretation of the references to colour in this figure legend, the reader is referred to the Web version of this article.)

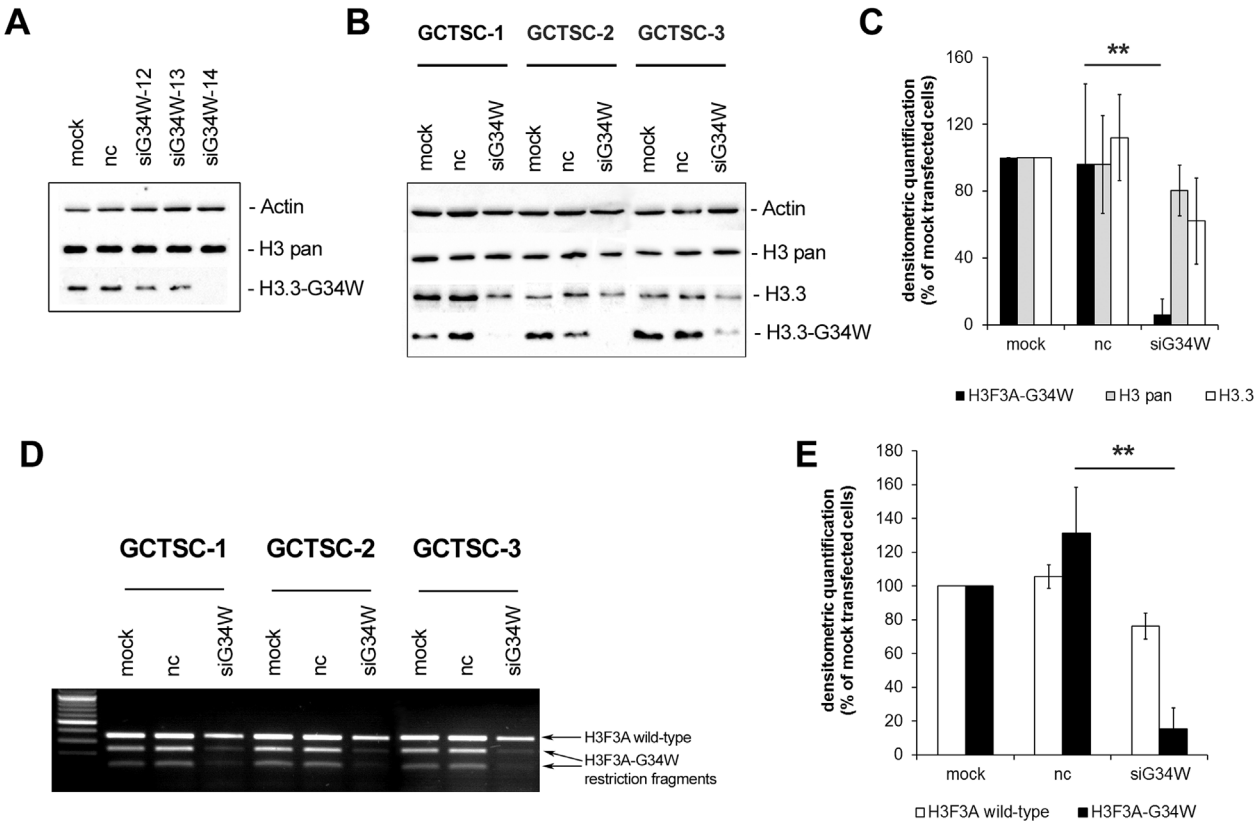

Fig. 3. Specific siRNA mediated knockdown of H3.3-G34W. **(A)** Western blot analysis of the H3.3-G34W knockdown efficiency of different siRNAs 12 days after transient transfection. Actin has been detected as loading control. **(B)** Western blot analysis of siRNA mediated H3.3-G34W knockdown in GCTSC cell lines used for further experiments. **(C)** Densitometric quantification of total H3, H3.3 and H3.3-G34W levels shown in **(B)**. Data were normalized to the reference protein actin and are presented as percent of mock transfected cells. **(D)** Analysis of H3F3A transcripts by restriction site mutation analysis of amplified cDNA fragments spanning the mutated site in *H3F3A*. **(E)** Densitometric quantification of the restriction fragments shown in C (**p < 0.01).

In contrast, a significant knockdown to 5.9% compared to mock transfected cells was observed for H3.3-G34W protein levels in all siG34W transfected cell lines. These data indicate a specific knockdown of H3.3-G34W while the expression of wild-type H3.3 is not or only slightly affected (Fig. 3B and C). Transcript levels of wild-type *H3F3A* and the mutated *H3F3A allele* were analyzed by restriction site analysis of PCR amplified cDNA fragments spanning the mutation site. While the uncut *H3F3A* wild-type fragment and the *H3F3A*-mutant specific restriction fragments could be detected in equal amounts in mock transfected cells and cells transfected with a negative control siRNA, fragments representing the mutated allele were significantly downregulated in siG34W transfected cells to 15% compared to mock transfected cells (Fig. 3 D and E).

3.4. H3F3A-G34W knockdown significantly inhibits cell proliferation

As we already observed an increased proliferation of H3.3 G34W stromal cells compared to H3.3 wild-type stromal cells [16] we asked whether a knockdown of H3.3 G34W expression could decrease proliferation. To this end, GCTSC cell lines were transiently transfected with siG34W and split into 96-well plates 48 h after transfection. Quantification of cell numbers over a period of 9 days showed a significantly decreased cell proliferation of siG34W transfected cells compared to control cells. As controls either mock transfected cells without the addition of siRNA or cells transfected with a non-targeting siRNA control were used (Fig. 4).

3.5. H3.3-G34W knockdown significantly inhibits cell migration

In addition to an increased proliferation, H3.3 G34W positive cells are further characterized by an increased migration capacity compared to H3.3 wild-type cells [16]. To verify whether the expression of H3.3 G34W is responsible for this observation GCTSCs were transfected with siG34W and plated in 96-well plates with a defined cell-free area of 2 mm diameter. Cells were allowed to migrate for 48 h before they were stained with calcein-AM and photographed. Quantification of the populated migration area showed that the H3.3-G34W knockdown reduced the migration capacity of three individual GCTSC cell lines to 35%, 34% and 24% respectively compared to mock transfected cells (Fig. 5 A and B) and proofed a direct influence of H3.3 G34W expression on migration capacity, an important feature of neoplastic transformation.

3.6. Colony formation capacity is significantly reduced in siG34W transfected GCTSCs

The ability to proliferate and to form colonies in semi-solid matrices is a key feature of tumor cells. We therefore analyzed the influence of H3.3-G34W knockdown on the colony forming capacity of GCTSCs. Transient siG34W transfection of three GCTSCS significantly reduced the number of colonies to 46%, 53% and 30% compared to mock transfected cells. In addition to the amount also the size of the colonies was reduced what might be explained by reduced proliferation as shown in Fig. 4 (Fig. 6 A and B).

3.7. Knockdown of H3.3-G34W inhibits RANKL mRNA expression of GCTSCs

Recruitment of giant cell precursors and the formation of osteoclast-like giant cells is a key feature in GCTs. A central role in this process

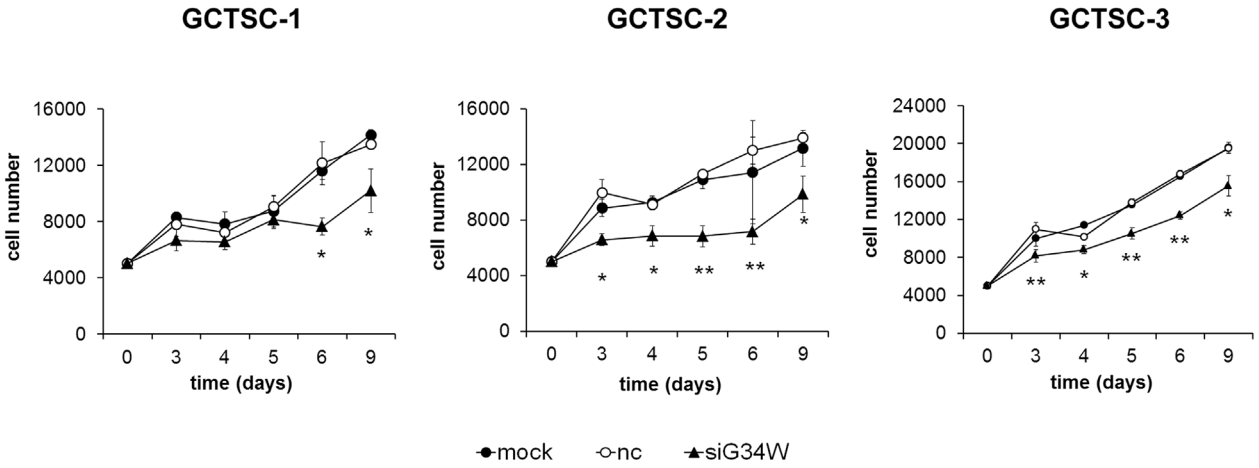

Fig. 4. Influence of H3.3-G34W knockdown on cell proliferation. GCTSCs were transiently transfected with siG34W and cell numbers were quantified at the indicated time points. Experiments were done in triplicates. (mock = transfection without addition of siRNA; nc = negative control siRNA; **p < 0.01; *p < 0.05).

plays the secretion of receptor activator of NF-κB ligand (RANKL) by the neoplastic stromal cells. We therefore investigated the mRNA expression of RANKL in GCTSCs after H3.3-G34W knockdown and observed a significant reduction to 57% compared to mock transfected cells (Fig. 6C).

3.8. H3.3-G34W knockdown inhibits tumor engraftment and growth in vivo

To analyze the effects of a H3.3-G34W knockdown on tumor growth *in vivo* we used a chicken chorionallantoic membrane (CAM) model. Tumor cells transfected with siG34W, a negative control siRNA and mock transfected cells were inoculated onto the CAM of fertilized chicken eggs. The high degree of vascularization and the provided extracellular matrix proteins mimic the physiological cancer environment and make the CAM an ideal substrate for the cultivation of tumor cells. Grafting of tumors is further facilitated by a natural immunodeficiency of the chicken embryo until developmental day 14. H3.3-G34W knockdown significantly reduced the tumor take rates and the tumor volumes compared to the control cells. The analysis of three GCTSC cell lines showed a reduction of tumor volumes to 63%, 50% and 36% compared to mock transfected cells (Fig. 7A). In addition, the tumor take rates were reduced to 40%, 77% and 68% compared to the corresponding mock transfected cells resulting in an overall decrease of the cumulative tumor volumes to 42%, 29% and 18% respectively (Fig. 7 B, C and D). No significant effect could be observed after transfection with a negative control siRNA.

4. Discussion

Histones are crucial for the organization and maintenance of the chromatin structure. In addition to the nucleosome mediated condensation of DNA multiple, post translational modifications of the N-terminal tail of the histone molecules modulate the accessibility of the DNA, thus affecting genomic stability and transcriptional regulation. Disturbance of this fine-tuned system leads to loss of genomic integrity, alterations in the epigenetic landscape and as a consequence to the development of cancer [17]. Recurrent histone mutations are often associated with further somatic mutations including the chromatin remodeling genes *ATRX* and *DAXX* [10], *TP53* (tumor protein p53) [18], *NF1* (neurofibromin 1) [19] and *PDGFRA* (platelet-derived growth factor receptor, alpha) [20]. In GCTB however, except H3.3-G34W no additional recurrent genetic alterations can be detected. Further, in contrast to H3.3-K27M and H3.3-K36M, H3.3-G34W does not affect an amino acid that is a direct target for histone modification.

In a previous study we observed a significant elevation of cell proliferation, infiltrative capacity and colony formation in H3.3-G34W cells compared to H3.3 wild-type cells isolated from GCTB tissue [16]. The question, whether this single heterozygous mutation encoding the oncohistone H3.3-G34W is sufficient to drive increased proliferation and tumorigenesis in GCTB was addressed in this study. In a cohort of 84 GCTB patients we could detect H3.3-G34W in 79 cases (94%). We assume that this percentage might even be higher due to misdiagnoses of giant cell rich lesions with similar histology. In addition to PCR and western-blot analysis we used a restriction enzyme based method to detect H3.3-G34W that turned out to be an accurate, reliable and cost

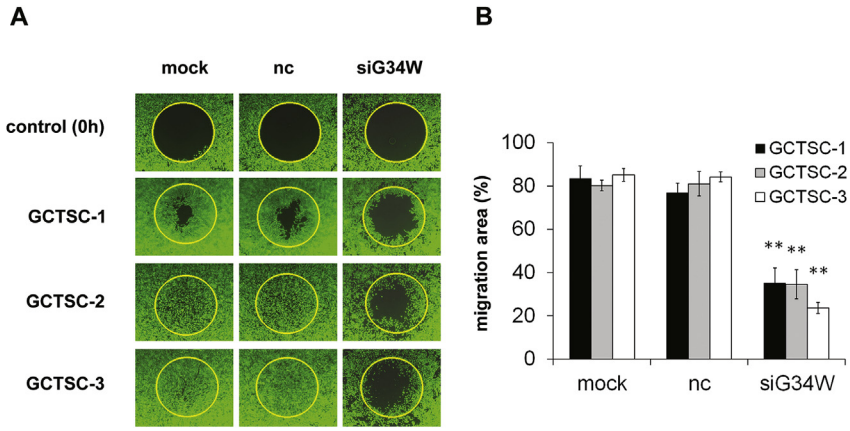

Fig. 5. H3.3-G34W knockdown inhibits cell migration capacity of GCTSCs. **(A)** Representative photographs of calcein-AM stained GCTSCs after 48 h of migration. The initial cell-free area is outlined in yellow. **(B)** Quantification of the populated migration area. (mock = transfection without addition of siRNA; nc = negative control siRNA; **p < 0.01). (For interpretation of the references to colour in this figure legend, the reader is referred to the Web version of this article.)

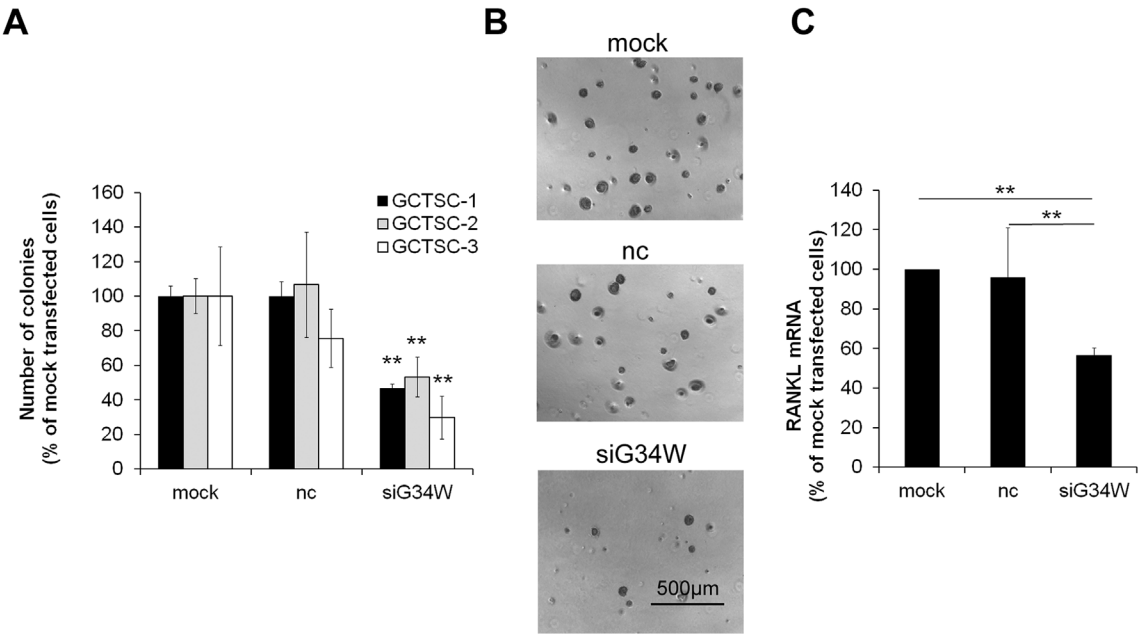

Fig. 6. Impact of H3.3-G34W knockdown on the colony forming capacity of GCTSCs and RANKL mRNA expression. **(A)** Relative number of colonies formed after 28 days culture in 0.3% agar. Numbers are expressed as % of mock transfected cells. **(B)** Representative photographs of colonies formed by GCTSCs cultured in 0.3% agar (mock = transfection without addition of siRNA; nc = negative control siRNA). **(C)** RANKL mRNA expression in GCTSCs (n = 5) 72 after siG34W transfection. Expression values were normalized to the expression of the reference gene RPS13 in the corresponding sample (**p < 0.01).

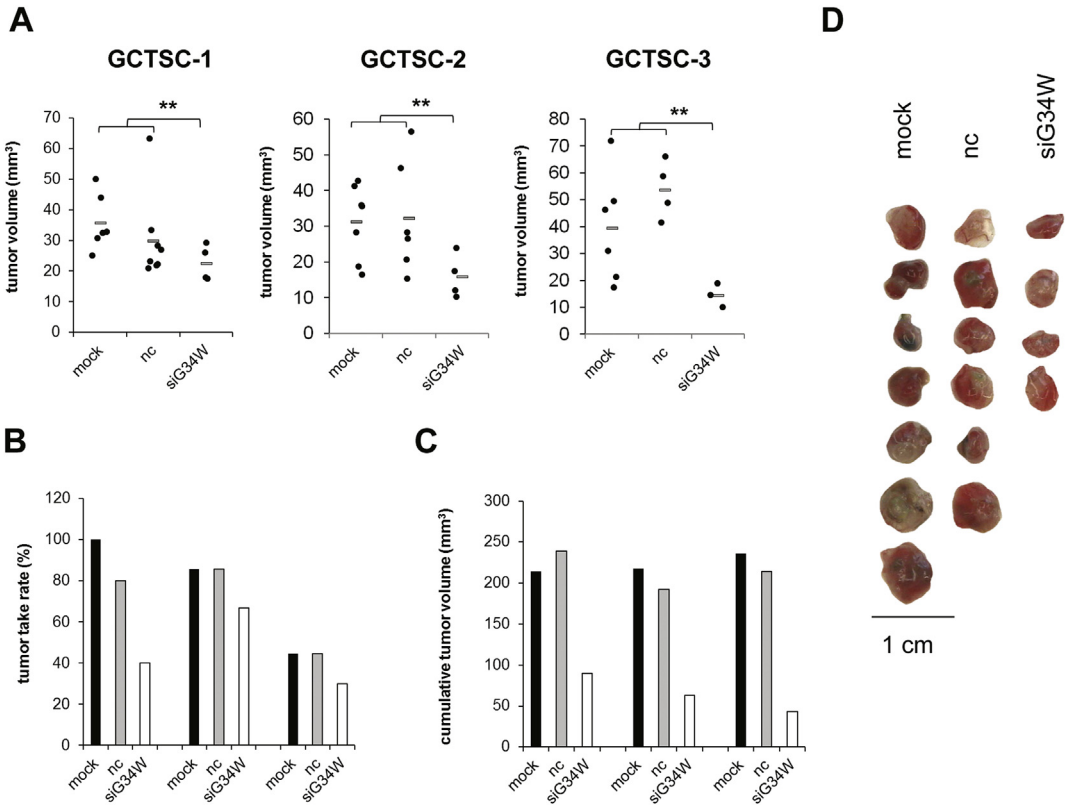

Fig. 7. Knockdown of H3.3-G34W significantly inhibits tumor engraftment and growth *in vivo*. **(A)** GCTSC cell lines (n = 3) were transfected with siG34W, a negative control siRNA (nc) or without the addition of siRNA (mock) and transplanted onto the CAM of fertilized chicken eggs. After seven days tumors that formed were resected and the tumor volumes were quantified. **(B)** Calculated tumor take rates. Chicken embryos that died before developmental day 16 were excluded. **(C)** Cumulative tumor volumes of all tumors formed in one experimental group. **(D)** Representative photographs of tumor xenografts of each treatment group (**p < 0.01).

effective screening tool that might be useful for diagnostic purposes. Using a siRNA based approach we could demonstrate that H3.3-G34W knockdown significantly alters the neoplastic phenotype of GCTSCs including inhibition of proliferation, migration and colony forming capacity. Xenotransplantation of GCTSCs further confirmed a significant impact of H3.3-G34W knockdown on tumor engraftment and growth *in vivo*. These data indicate that the oncohistone H3.3-G34W is sufficient to drive tumorigenesis in GCTB. However, the precise mechanisms by which this alteration in the *H3F3A* gene might drive tumorigenesis are still not fully understood.

The lysine to methionine substitutions H3.3-K27M and H3.3-K36M found in other tumor entities have been shown to promote tumorigenesis mainly by mechanisms affecting the genome wide methylation pattern. Either inactivation of PRC2 (polycomb repressive complex 2) causes a global loss of the repressive chromatin mark H3K27me3 [21] or H3K36 trimethylation is globally reduced due to a H3.3-K36M mediated inhibition of methyltransferases MMSET/NSD2 (multiple myeloma SET domain/Nuclear SET Domain-Containing Protein 2) and SETD2 (SET domain containing 2) [22,23]. In contrast, the molecular consequences of G34 mutations are less well understood. Although the glycine at position 34 is not post-translationally modified a substitution of this amino acid might influence K36 accessibility and methylation due to its close proximity which then mediates epigenetic changes. Indeed, H3G34 V/R/D mutations have been shown to block H3K36 methylation and interactions of H3K36me3 with the mismatch repair protein MutSα resulting in genome instability and elevated mutation frequencies [24]. While stable expression of H3.3-G34W in HeLa cells provoked no global effects on H3 methylation, reduced levels of H3K36me3 a marker of actively transcribed genes and increased levels of H3K27me3 a repressive marker have been observed in ectopic H3.3 indicating effects of H3.3-G34W in cis on the same histone tail [25]. Likewise, compared to *H3F3A* wild-type cells no global changes in H3K36 trimethylation could be detected in the glioblastoma cell line KNS42 harbouring a G34V mutation. However, a differential binding pattern of this activating mark could be detected that affects the expression of numerous transcription factors including the proto-oncogene *MYCN* (myelocytomatosis viral related oncogene, neuroblastoma derived). Mutations affecting G34 have thus been suggested to represent an alternative mechanism to increase MYCN expression [26]. In addition to epigenetic alterations, H3.3-G34W has been shown to interact with components of the spliceosome and RNA processing machinery that might further drive the process of neoplastic transformation [16].

In summary, we could selectively knockdown H3.3-G34W in GCTSCs with fundamental consequences for the neoplastic phenotype of these cells. Significant inhibition of proliferation, migration and colony formation *in vitro* and reduced tumor engraftment and growth *in vivo* verified that the single H3.3-G34W mutation is sufficient to drive tumorigenesis in GCTB. However, loss of wild-type H3.3 itself has been shown to induce considerable changes in chromatin assessment and gene expression [27]. A global reduction of wild-type H3.3 levels caused by the mutation of one H3.3 coding allele in GCTB might thus contribute to tumorigenesis as well. Further, in this study the effects of H3.3-G34W knockdown have only been studied on the neoplastic stromal cell population and not the other cell types found in GCTB, especially the osteoclast-like giant cells that are responsible for the osteolytic defects and bone destructions observed in GCTB patients. Although our observation of a reduced RANKL expression in H3.3G34W knockdown cells suggests that osteoclast formation and activity might also be reduced, the use of oncohistone H3.3-G34W as therapeutic target requires further studies on this important aspect of GCTB development.

Conflicts of interest

There are no conflicts of interest to declare.

Acknowledgements

This study was funded in part by Deutsche Krebshilfe, Germany (grant 111298).

References

[1] B.J. Noh, Y.K. Park, Giant cell tumor of bone: updated molecular pathogenesis and tumor biology, Hum. Pathol. 81 (2018) 1–8.
[2] K.A. Raskin, J.H. Schwab, H.J. Mankin, D.S. Springfield, F.J. Hornicek, Giant cell tumor of bone, J. Am. Acad. Orthop. Surg. 21 (2013) 118–126.
[3] W.T. Becker, J. Dohle, L. Bernd, A. Braun, M. Cserhati, A. Enderle, L. Hovy, Z. Matejovsky, M. Szendroi, K. Trieb, P.U. Tunn, Local recurrence of giant cell tumor of bone after intralesional treatment with and without adjuvant therapy, J. Bone Joint Surg. Am. 90 (2008) 1060–1067.
[4] S. Behjati, P.S. Tarpey, N. Presneau, S. Scheipl, N. Pillay, P. Van Loo, D.C. Wedge, S.L. Cooke, G. Gundem, H. Davies, S. Nik-Zainal, S. Martin, S. McLaren, V. Goodie, B. Robinson, A. Butler, J.W. Teague, D. Halai, B. Khatri, O. Myklebost, D. Baumhoer, G. Jundt, R. Hamoudi, R. Tirabosco, M.F. Amary, P.A. Futreal, M.R. Stratton, P.J. Campbell, A.M. Flanagan, Distinct H3F3A and H3F3B driver mutations define chondroblastoma and giant cell tumor of bone, Nat. Genet. 45 (2013) 1479–1482.
[5] J. Fullgrabe, E. Kavanagh, B. Joseph, Histone onco-modifications, Oncogene 30 (2011) 3391–3403.
[6] L. Qiu, X. Hu, Q. Jing, X. Zeng, K.M. Chan, J. Han, Mechanism of cancer: oncohistones in action, J. Genet. Genomics. 45 (2018) 227–236.
[7] I. Maze, K.M. Noh, A.A. Soshnev, C.D. Allis, Every amino acid matters: essential contributions of histone variants to mammalian development and disease, Nat. Rev. Genet. 15 (2014) 259–271.
[8] E. Delbarre, K. Ivanauskiene, T. Kuntziger, P. Collas, DAXX-dependent supply of soluble (H3.3-H4) dimers to PML bodies pending deposition into chromatin, Genome Res. 23 (2013) 440–451.
[9] A.D. Goldberg, L.A. Banaszynski, K.M. Noh, P.W. Lewis, S.J. Elsaesser, S. Stadler, S. Dewell, M. Law, X. Guo, X. Li, D. Wen, A. Chapgier, R.C. DeKelver, J.C. Miller, Y.L. Lee, E.A. Boydston, M.C. Holmes, P.D. Gregory, J.M. Greally, S. Rafii, C. Yang, P.J. Scambler, D. Garrick, R.J. Gibbons, D.R. Higgs, I.M. Cristea, F.D. Urnov, D. Zheng, C.D. Allis, Distinct factors control histone variant H3.3 localization at specific genomic regions, Cell 140 (2010) 678–691.
[10] J. Schwartzentruber, A. Korshunov, X.Y. Liu, D.T. Jones, E. Pfaff, K. Jacob, D. Sturm, A.M. Fontebasso, D.A. Quang, M. Tonjes, V. Hovestadt, S. Albrecht, M. Kool, A. Nantel, C. Konermann, A. Lindroth, N. Jager, T. Rausch, M. Ryzhova, J.O. Korbel, T. Hielscher, P. Hauser, M. Garami, A. Klekner, L. Bognar, M. Ebinger, M.U. Schuhmann, W. Scheurlen, A. Pekrun, M.C. Fruhwald, W. Roggendorf, C. Kramm, M. Durken, J. Atkinson, P. Lepage, A. Montpetit, M. Zakrzewska, K. Zakrzewski, P.P. Liberski, Z. Dong, P. Siegel, A.E. Kulozik, M. Zapatka, A. Guha, D. Malkin, J. Felsberg, G. Reifenberger, A. von Deimling, K. Ichimura, V.P. Collins, H. Witt, T. Milde, O. Witt, C. Zhang, P. Castelo-Branco, P. Lichter, D. Faury, U. Tabori, C. Plass, J. Majewski, S.M. Pfister, N. Jabado, Driver mutations in histone H3.3 and chromatin remodelling genes in paediatric glioblastoma, Nature 482 (2012) 226–231.
[11] S. Papillon-Cavanagh, C. Lu, T. Gayden, L.G. Mikael, D. Bechet, C. Karamboulas, L. Ailles, J. Karamchandani, D.M. Marchione, B.A. Garcia, I. Weinreb, D. Goldstein, P.W. Lewis, O.M. Dancu, S. Dhaliwal, W. Stecho, C.J. Howlett, J.S. Mymryk, J.W. Barrett, A.C. Nichols, C.D. Allis, J. Majewski, N. Jabado, Impaired H3K36 methylation defines a subset of head and neck squamous cell carcinomas, Nat. Genet. 49 (2017) 180–185.
[12] H. Li, M.S. Kaminski, Y. Li, M. Yildiz, P. Ouillette, S. Jones, H. Fox, K. Jacobi, K. Saiya-Cork, D. Bixby, D. Lebovic, D. Roulston, K. Shedden, M. Sabel, L. Marentette, V. Cimmino, A.E. Chang, S.N. Malek, Mutations in linker histone genes HIST1H1 B, C, D, and E; OCT2 (POU2F2); IRF8; and ARID1A underlying the pathogenesis of follicular lymphoma, Blood 123 (2014) 1487–1498.
[13] C. Koelsche, D. Schrimpf, L. Tharun, E. Roth, D. Sturm, D.T.W. Jones, E.K. Renker, M. Sill, A. Baude, F. Sahm, D. Capper, M. Bewerunge-Hudler, W. Hartmann, A.E. Kulozik, I. Petersen, U. Flucke, H.W.B. Schreuder, R. Buttner, M.A. Weber, P. Schirmacher, C. Plass, S.M. Pfister, A. von Deimling, G. Mechtersheimer, Histone 3.3 hotspot mutations in conventional osteosarcomas: a comprehensive clinical and molecular characterization of six H3F3A mutated cases, Clin. Sarcoma Res. 7 (2017) 9.
[14] J. Rehkamper, K. Steinestel, B. Jeiler, S. Elges, E. Hekeler, S. Huss, J. Sperveslage, J. Hardes, A. Streitburger, G. Gosheger, E. Wardelmann, D. Baumhoer, M. Trautmann, W. Hartmann, Diagnostic tools in the differential diagnosis of giant cell-rich lesions of bone at biopsy, Oncotarget 9 (2018) 30106–30114.
[15] I.M. Schaefer, J.A. Fletcher, G.P. Nielsen, A.R. Shih, M.L. Ferrone, J.L. Hornick, X. Qian, Immunohistochemistry for histone H3G34W and H3K36M is highly specific for giant cell tumor of bone and chondroblastoma, respectively, FNA and Core Needle Biopsy, Cancer Cytopathol, 2018.
[16] J. Lim, J.H. Park, A. Baude, Y. Yoo, Y.K. Lee, C.R. Schmidt, J.B. Park, J. Fellenberg, J. Zustin, F. Haller, I. Krucken, H.G. Kang, Y.J. Park, C. Plass, A.M. Lindroth, The histone variant H3.3 G34W substitution in giant cell tumor of the bone link chromatin and RNA processing, Sci. Rep. 7 (2017) 13459.
[17] F. Mohammad, K. Helin, Oncohistones: drivers of pediatric cancers, Genes Dev. 31 (2017) 2313–2324.
[18] H. Nikbakht, E. Panditharatna, L.G. Mikael, R. Li, T. Gayden, M. Osmond, C.Y. Ho, M. Kambhampati, E.I. Hwang, D. Faury, A. Siu, S. Papillon-Cavanagh, D. Bechet,

K.L. Ligon, B. Ellezam, W.J. Ingram, C. Stinson, A.S. Moore, K.E. Warren, J. Karamchandani, R.J. Packer, N. Jabado, J. Majewski, J. Nazarian, Spatial and temporal homogeneity of driver mutations in diffuse intrinsic pontine glioma, Nat. Commun. 7 (2016) 11185.

[19] K. Aihara, A. Mukasa, K. Gotoh, K. Saito, G. Nagae, S. Tsuji, K. Tatsuno, S. Yamamoto, S. Takayanagi, Y. Narita, S. Shibui, H. Aburatani, N. Saito, H3F3A K27M mutations in thalamic gliomas from young adult patients, Neuro Oncol. 16 (2014) 140–146.

[20] W.A. Flavahan, Y. Drier, B.B. Liau, S.M. Gillespie, A.S. Venteicher, A.O. Stemmer-Rachamimov, M.L. Suva, B.E. Bernstein, Insulator dysfunction and oncogene activation in IDH mutant gliomas, Nature 529 (2016) 110–114.

[21] P.W. Lewis, M.M. Muller, M.S. Koletsky, F. Cordero, S. Lin, L.A. Banaszynski, B.A. Garcia, T.W. Muir, O.J. Becher, C.D. Allis, Inhibition of PRC2 activity by a gain-of-function H3 mutation found in pediatric glioblastoma, Science 340 (2013) 857–861.

[22] D. Fang, H. Gan, J.H. Lee, J. Han, Z. Wang, S.M. Riester, L. Jin, J. Chen, H. Zhou, J. Wang, H. Zhang, N. Yang, E.W. Bradley, T.H. Ho, B.P. Rubin, J.A. Bridge, S.N. Thibodeau, T. Ordog, Y. Chen, A.J. van Wijnen, A.M. Oliveira, R.M. Xu, J.J. Westendorf, Z. Zhang, The histone H3.3K36M mutation reprograms the epigenome of chondroblastomas, Science 352 (2016) 1344–1348.

[23] C. Lu, S.U. Jain, D. Hoelper, D. Bechet, R.C. Molden, L. Ran, D. Murphy, S. Venneti, M. Hameed, B.R. Pawel, J.S. Wunder, B.C. Dickson, S.M. Lundgren, K.S. Jani, N. De Jay, S. Papillon-Cavanagh, I.L. Andrulis, S.L. Sawyer, D. Grynspan, R.E. Turcotte, J. Nadaf, S. Fahiminiyah, T.W. Muir, J. Majewski, C.B. Thompson, P. Chi, B.A. Garcia, C.D. Allis, N. Jabado, P.W. Lewis, Histone H3K36 mutations promote sarcomagenesis through altered histone methylation landscape, Science 352 (2016) 844–849.

[24] J. Fang, Y. Huang, G. Mao, S. Yang, G. Rennert, L. Gu, H. Li, G.M. Li, Cancer-driving H3G34V/R/D mutations block H3K36 methylation and H3K36me3-MutSalpha interaction, Proc. Natl. Acad. Sci. U. S. A. 115 (2018) 9598–9603.

[25] L. Shi, J. Shi, X. Shi, W. Li, H. Wen, Histone H3.3 G34 mutations alter histone H3K36 and H3K27 methylation in cis, J. Mol. Biol. 430 (2018) 1562–1565.

[26] L. Bjerke, A. Mackay, M. Nandhabalan, A. Burford, A. Jury, S. Popov, D.A. Bax, D. Carvalho, K.R. Taylor, M. Vinci, I. Bajrami, I.M. McGonnell, C.J. Lord, R.M. Reis, D. Hargrave, A. Ashworth, P. Workman, C. Jones, Histone H3.3. mutations drive pediatric glioblastoma through upregulation of MYCN, Cancer Discov. 3 (2013) 512–519.

[27] H.T. Fang, C.A. El Farran, Q.R. Xing, L.F. Zhang, H. Li, B. Lim, Y.H. Loh, Global H3.3 dynamic deposition defines its bimodal role in cell fate transition, Nat. Commun. 9 (2018) 1537.